Journal of Alloys and Compounds 509 (2011) 8894–8900

Contents lists available at ScienceDirect

Journal of Alloys and Compounds

journal homepage: www.elsevier.com/locate/jallcom

Fabrication and properties of $Ba(Zr_{1-x}Ce_x)_{0.9}Y_{0.1}O_{2.95}$/NaCl composite electrolyte materials

Ruisong Guo*, Yaping Deng, Yanying Gao, Lixin Zhang

Key Laboratory of Advanced Ceramics and Machining Technology, Ministry of Education, Tianjin University, Tianjin 300072, China

ARTICLE INFO

Article history:
Received 4 March 2011
Received in revised form 31 May 2011
Accepted 1 June 2011
Available online 25 June 2011

Keywords:
Sintering
Composite materials
Fuel cells
Ionic conduction
Electrical transport

ABSTRACT

$Ba(Zr_{1-x}Ce_x)_{0.9}Y_{0.1}O_{2.95}$/NaCl ($x = 0.1$, 0.2 and 0.3) composite electrolyte materials were fabricated with ZnO as sintering aid. The effect of ZnO on the properties of $Ba(Zr_{1-x}Ce_x)_{0.9}Y_{0.1}O_{2.95}$ matrix were investigated. The phase composition and microstructure of samples were characterized by XRD and SEM, respectively. The electrochemical performances were studied by three-probe conductivity measurement and AC impedance spectroscopy. XRD results showed that $Ba(Zr_{1-x}Ce_x)_{0.9}Y_{0.1}O_{2.95}$ with 2 mol% of ZnO was perovskite structure. The relative density of this sample was above 95% when sintered at 1450 °C for 6 h. By adding 10 mol% of NaCl to $Ba(Zr_{1-x}Ce_x)_{0.9}Y_{0.1}O_{2.95}$ with 2 mol% of ZnO that was sintered at 1400 °C for 6 h, the conductivity was increased. The electrical conductivity of 1.26×10^{-2} S/cm and activation energy of 0.23 eV were obtained when tested at 800 °C in wet hydrogen.

1. Introduction

Many perovskite-type oxides have been reported for their high proton conductivity at temperatures ranging from 500 °C to 800 °C. Yttrium-doped perovskite $BaZrO_3$ (BZY) ceramics [1–4] have been widely studied for their potential applications in proton ceramic fuel cells (PCFCs) and other fields. During the past several years, the investigations of proton conductors in perovskite ceramics were mainly focused on single-phase cerates or zirconates, such as doped $BaCeO_3$ [5–7] or doped $BaZrO_3$ [8,9]. Doped $BaCeO_3$ does not require a very high sintering temperature and exhibits high proton conductivity. However, it is unstable in CO_2/H_2O containing atmosphere. Doped $BaZrO_3$, on the other hand, is much more stable in atmosphere containing CO_2 and H_2O, but its poor sinterability requires very high sintering temperature. $BaZrO_3$ usually exhibits a fine-grained microstructure, even sintered at >1700 °C for a long time [10,11]. There is a large fraction of grain boundary in such a fine-grained material. $BaZrO_3$ has high bulk conductivity, but it has low grain boundary conductivity, which is three to four orders of magnitude lower than the former. This greatly limited the applications of $BaZrO_3$ materials. Peng et al. [12] reported $BaZrO_3$ proton conductor with grain size of only several hundred nanometers sintered at 1600 °C with long soaking time. A relatively low conductivity which was only $10^{-2.4}$ to 10^{-3} S/cm at 700 °C has been observed due to the large amount of grain boundary. Xu et al. [13] synthesized $Ba_{0.95}K_{0.05}Zr_{0.85}Y_{0.11}Zn_{0.04}O_{3-\delta}$ using a conventional solid-state reaction method. The density of the sample reached 92% of its theoretical density. They suggested that introducing extra potassium led to the formation of second phase. The maximum power density and conductivity reached 7.7 mW/cm^2 and 0.006 S/cm respectively at 718 °C. Sun et al. [14] employed a co-pressing and co-firing method to fabricate a BZY membrane on a NiO–$BaZr_{0.1}Ce_{0.7}Y_{0.2}O_{3-\delta}$ (NiO–BZCY) anode substrate at a relatively low sintering temperature of 1400 °C and a maximum power density of 170 mW/cm^2 was obtained at 700 °C. Park et al. [15] fabricated the $Ba(Zr_{1-x}Yb_x)O_{3-\delta} + y$CuO by solid-state reactions. They reported that the sintered density of the composite with 1.0 mol% of CuO reached up to 99% of its theoretical density at 1500 °C.

Recently, Y-doped $BaCe_xZr_{1-x}O_{3-\delta}$ (BZCY) composites [16–20] also have been studied and some additives were added to improve the sintering behavior [21,22]. Guo et al. [23] reported enhanced sinterability of $BaZr_{0.4}Ce_{0.4}Y_{0.2}O_{3-\delta}$ with ZnO as a sintering aid. The relative density reached 95% after sintering at 1450 °C for 5 h. Their results demonstrated that ZnO is one of the most effective sintering aids to densify the ceramics. Wang et al. [24] researched sintering behavior and conductivity of yttrium-doped $BaCeO_3$–$BaZrO_3$ solid solutions using ZnO additive. The results given by several authors also pointed out that excessive sintering aid could lower the electrical conductivity [15,22,24].

In order to decrease the sintering temperature and to increase the total conductivity, the strategy of combining $BaZrO_3$ with $BaCeO_3$ is considered in the present work. It is expected that

* Corresponding author. Tel.: +86 22 27404262; fax: +86 22 27404724.
E-mail address: rsguo@tju.edu.cn (R. Guo).

0925-8388/$ – see front matter © 2011 Elsevier B.V. All rights reserved.
doi:10.1016/j.jallcom.2011.06.004

the shortcomings of $BaZrO_3$ [25] can be partially compensated by $BaCeO_3$ [26]. The amount of $BaCeO_3$ introduced should be limited to an extent without sacrificing the chemical stability of $BaZrO_3$ to CO_2/H_2O containing atmosphere. Moreover, the grain boundary conductivity must be effectively improved in order to further increase the total conductivity of the composite. One way is to add inorganic salts with proton conduction to the composite. The salt is homogeneously dispersed along the grain boundary, which can be transformed to super-ionic phase [27,28] and enhance the proton migration rate along the grain boundary. As a result, high conductivities of the composite can be achieved. However, high sintering temperature of $BaZrO_3$–$BaCeO_3$ composite is not compatible with either the evaporation or decomposition temperature of salts. Therefore, the sintering temperature of composite must be lowered.

In this work, the $Ba(Zr_{1-x}Ce_x)_{0.9}Y_{0.1}O_{2.95}$ (x = 0.1, 0.2, 0.3, named as BZCY series) was first prepared as the matrix. The effect of x on the sintering temperature and conductivity of the materials were investigated. Then, the effect of ZnO on the sintering behavior and electrical conductivity of $Ba(Zr_{1-x}Ce_x)_{0.9}Y_{0.1}O_{2.95}$ were studied, based on the optimized composition of BZCY series. Finally, NaCl was added into the $Ba(Zr_{1-x}Ce_x)_{0.9}Y_{0.1}O_{2.95}$ + ZnO as the second phase to obtain the composite electrolyte material. The total conductivity and the effect of NaCl were studied by three-probe DC conductivity and AC impedance measurements.

2. Experimental details

The raw materials used in this work are $BaCO_3$ (99.5%, Standard Science and Technology Company of Tianjin, China), ZrO_2 (99.5%, Yuelong New Materials Company of Shanghai, China), CeO_2 (99.5%, Xinhua Chemical Reagent Company of Beijing, China), Y_2O_3 (99.95%, Yuelong New Materials Company of Shanghai, China), ZnO (99.0%, Jiangtian Reagent Company of Tianjin, China) and NaCl (99.5%, Jiangtian Reagent Company of Tianjin, China). $Ba(Zr_{1-x}Ce_x)_{0.9}Y_{0.1}O_{2.95}$ (x = 0.1, 0.2 and 0.3, named as BZCY series) powders were synthesized by solid-state reaction route. $BaCO_3$, ZrO_2, CeO_2 and Y_2O_3 were ball milled with ethanol as media for 8 h. The resultant mixture was dried, followed by calcination at 1300 °C for 4 h. ZnO was then added to the calcined BZCY powders. Powders were ball milled again in ethanol for 8 h and then dried at 80 °C for 6 h. Finally, NaCl was added to BZCY–Z powders in a similar way. In the following discussions, BZCY–Z and BZCY–Z–Cl series stand for BZCY powders with addition of ZnO alone and ZnO together with NaCl, respectively. The detailed composition of the three series materials is listed in Table 1.

All the powders were pressed into disk pellets (13 mm in diameter and 2 mm in thickness) and sintered at 1600 °C for 4 h, 1450 °C for 6 h and 1400 °C for 6 h, respectively.

The density of the sintered samples was determined by Archimedes method and the relative density was calculated based on the theoretical density of $BaZrO_3$ (6.28 g/cm^{-3}) given by the PDF card No. 74-1299. At present, the theoretical densities of $Ba(Zr_{1-x}Ce_x)_{0.9}Y_{0.1}O_{2.95}$ with various x values are not available. The relative density was calculated just for a general comparison, rather than to evaluate their real extent of densification. The morphology and composition of fractured section of the sintered samples was characterized with a scanning electron microscope (SEM, XL-30ESEM, Philips, Netherlands) equipped with energy-dispersive X-ray analysis (EDX). To achieve a good electrode/electrolyte contact, Pt paste was applied on the surfaces of polished disks, followed by firing at 800 °C for 1 h. The electrical conductivities were measured by DC three-probe method with electrochemical workstation (CHI660C, Chenhua Instrument Company of Shanghai, China) in wet H_2 atmosphere (hydrogen passing through water with water vapor *ca.* 3%) at an interval of 50 °C in the temperature range from 600 to 800 °C. The AC impedance test was also carried out by the same way and the same equipment (frequency range from 0.1 Hz to 100 kHz, amplitude 30 mV).

3. Results and discussion

3.1. Densification of BZCY matrix

It has been widely reported that a high sintering temperature above 1700 °C is required for 10 mol% Y_2O_3 doped $BaZrO_3$ single-phase material. Peng et al. [12] reported that the relative density of 95% for the same material was obtained by sintering at 1600 °C with long soaking time of 8 h. It has also been noted it is not difficult for $BaCeO_3$ to be densified below 1600 °C by the solid-state reaction route [29]. It is therefore expected that the introduction of $BaCeO_3$ into $BaZrO_3$ may decrease the sintering temperature of the composite. The linear shrinkage and relative density of $Ba(Zr_{1-x}Ce_x)_{0.9}Y_{0.1}O_{2.95}$ (x = 0.1, 0.2, 0.3) sintered in air at 1600 °C for 4 h are shown in Fig. 1. It is clear that the linear shrinkage and relative density of samples exhibited a monotonous increase as increasing the value of x. Unfortunately, the maximum density is not high enough. Hence, the total conductivity of BZCY series materials is low. For example, the conductivities of BZCY2 and BZCY3 samples reached only 4.06×10^{-3} S/cm and 5.87×10^{-3} S/cm, respectively, in wet hydrogen atmosphere at 800 °C.

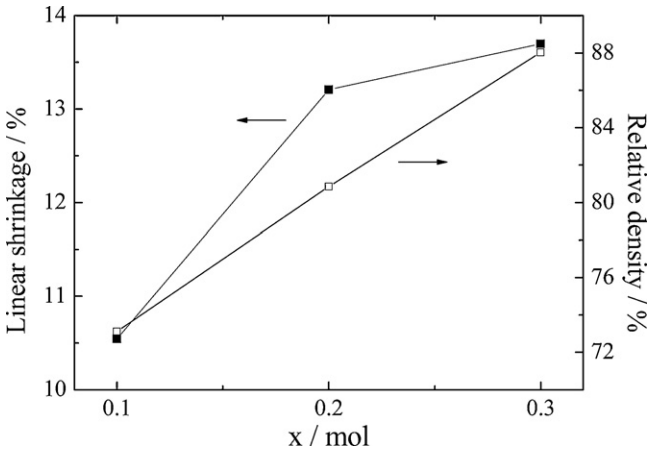

Fig. 1. Linear shrinkage and relative density of $Ba(Zr_{1-x}Ce_x)_{0.9}Y_{0.1}O_{2.95}$ (x = 0.1, 0.2, 0.3) after sintering in air at 1600 °C for 4 h.

3.2. Densification of BZCY3–Z composite electrolyte materials

To determine the sintering conditions of the BZCY3–Z series, the *in situ* linear shrinkage as a function of temperature was measured under an air atmosphere. The dilatometric curve of BZCY3–Z2 is shown in Fig. 2. The sample started to shrink at approximately 1241 °C. The total shrinkage is about 17.4% at the termination temperature of 1500 °C. Supposing the shrinkage of the sample in three dimensions is identical, the relative density of the tested sample can be roughly calculated to be 95.5% based on the total shrinkage (17.4%) and relative green density (53.8%). However, the shrinkage

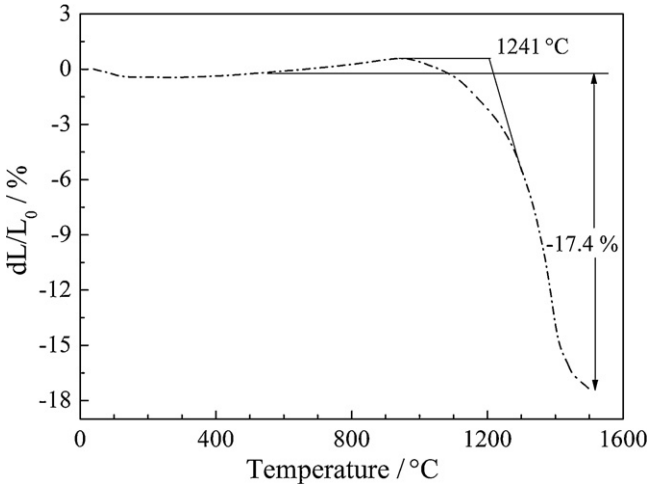

Fig. 2. Dilatometric curve of BZCY3–Z2 as a function of temperature.

Table 1
Composition of various series of composite electrolyte materials ($Ba(Zr_{1-x}Ce_x)_{0.9}Y_{0.1}O_{2.95}$).

Series	Sample name	x	BZCY3 (mol%)	ZnO (mol%)	BZCY3–Z2 (mol%)	NaCl (mol%)
BZCY	BZCY1	0.1				
	BZCY2	0.2				
	BZCY3	0.3				
BZCY3–Z	BZCY3–Z1		99	1		
	BZCY3–Z2		98	2		
	BZCY3–Z3		97	3		
	BZCY3–Z4		96	4		
BZCY3–Z2–Cl	BZCY3–Z2–Cl5				95	5
	BZCY3–Z2–Cl10				90	10
	BZCY3–Z2–Cl20				80	20

rate began to slow down after about 1400 °C. It is suggested that the samples might be densified around 1450 °C.

Fig. 3 shows the relative densities of the samples sintered at 1450 °C for 6 h. The sinterability of BZCY3–Z is much better than that of BZCY3. The relative density increased with increasing the content of ZnO and a 95% relative density was obtained for the sample by adding 2 mol% of ZnO. It is commonly believed that material with this density is basically suitable for an electrolyte of PCFCs. Enhanced sinterability was achieved with ZnO as a sintering aid, which is in good agreement with previous observations [20,24,30]. When the content of ZnO was increased to 4 mol%, the relative density of this sample is slightly higher than 96%. However, excessive ZnO might cause negative influences. It was reported that ZnO might evaporate at high temperatures [30] or form a liquid phase with Ba that evaporated during sintering [24], leaving holes in the sintered body. This is also proved by the microstructure observation shown in Fig. 4. Therefore, the sample with 2 mol% of ZnO was chosen for the following investigations.

The microstructure images of the fractured surface of BZCY3 (sintered at 1600 °C for 4 h) and BZCY3–Z2 (sintered at 1450 °C for 6 h) samples are shown in Fig. 4. BZCY3 exhibited a highly porous structure after firing at 1600 °C for 4 h. In contrast, BZCY3–Z2 pellet was almost completely densified after sintering at 1450 °C for 6 h. BZCY3 sample has fine and homogeneous grains with much narrower grain size distribution, even though it was sintered at a higher temperature than BZCY3–Z2 sample. When ZnO was added, the grain size increased and the porosity decreased, indicating that ZnO could promote the migration of grain boundary and densification during sintering. BZCY3–Z2 sample has large and inhomogeneous grains with wider grain size distribution. Large grains might have positive effect on electrical conductivity because the fraction of grain boundary decreases. This will be discussed in the following section.

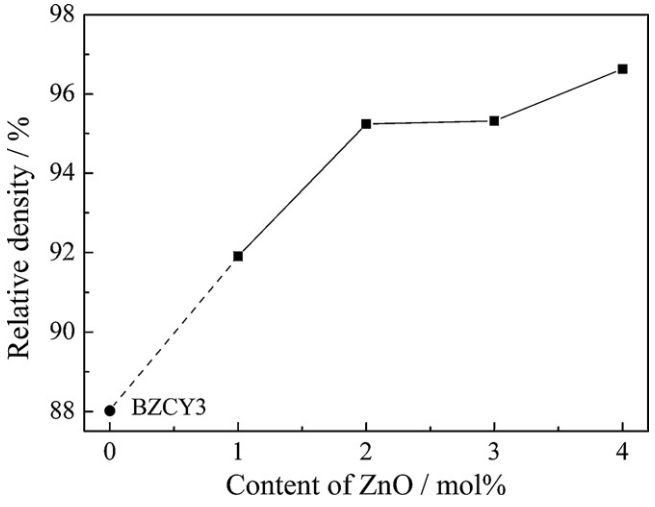

Fig. 3. Relativity density of BZCY3–Z after sintering at 1450 °C for 6 h. Relativity density of BZCY3 sintered at 1600 °C for 4 h is also given in this figure for comparison.

3.3. XRD characterizations of BZCY3–Z composite electrolyte materials

XRD pattern of BZCY3–Z2 sintered at 1450 °C for 6 h is shown in Fig. 5, along with the standard patterns of $BaZr_{0.9}Y_{0.1}O_{2.95}$ (PDF No. 04-011-7315) and $BaZr_{0.7}Ce_{0.2}Y_{0.1}O_{2.95}$ (PDF No. 04-011-7317). Single-phase cubic perovskite was obtained. All peaks for BZCY3–Z2 shifted to lower angles compared with the two standard patterns, indicating the increase of the unit cell. This is due to the bigger ionic radius of Ce^{4+} (R^{IV} = 0.092 nm) compared with that of Zr^{4+} (R^{IV} = 0.079 nm).

As can also be seen from Fig. 5, no impure phase was observed. ZnO phase was not detected in the BZCY3–Z2 sample although ZnO was added into the sample as an independent ingredient. This maybe because that the ZnO content is below detection limit of the diffractometer. Another possibility is that Zn^{2+} might partly dis-

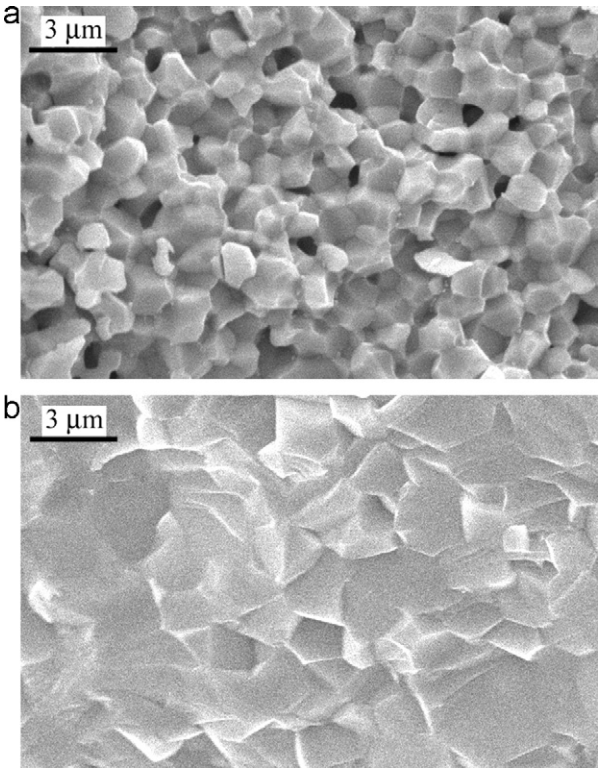

Fig. 4. Microstructure of the fractured surface of (a) BZCY3 sintered at 1600 °C for 4 h and (b) BZCY3–Z2 sintered at 1450 °C for 6 h.

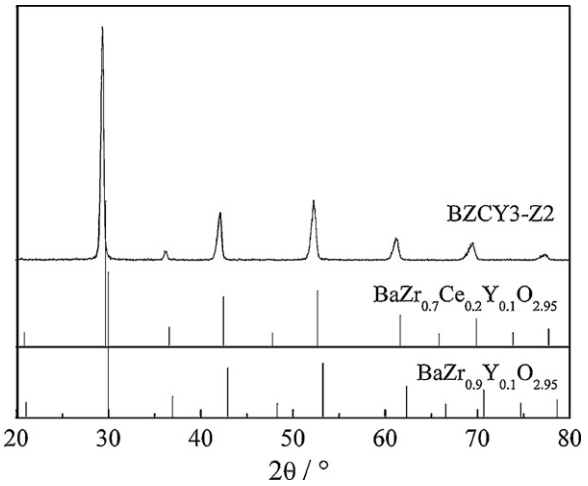

Fig. 5. XRD pattern of BZCY3–Z2 sintered at 1450 °C for 6 h as well as the standard patterns of $BaZr_{0.9}Y_{0.1}O_{2.95}$ and $BaZr_{0.7}Ce_{0.2}Y_{0.1}O_{2.95}$.

Table 2
Cell parameters of BZCY3–Z2, $BaZr_{0.9}Y_{0.1}O_{2.95}$ and $BaZr_{0.7}Ce_{0.2}Y_{0.1}O_{2.95}$.

Sample	$BaZr_{0.9}Y_{0.1}O_{2.95}$	$BaZr_{0.7}Ce_{0.2}Y_{0.1}O_{2.95}$	BZCY3–Z2
PDF card number	04-011-7315	04-011-7317	–
a (nm)	0.4211	0.4253	0.4278
Volume V (nm^3)	0.0747	0.0769	0.0783
ΔV (%)	−4.8	−1.8	0

solve into the lattice of $Ba(Zr_{0.7}Ce_{0.3})_{0.9}Y_{0.1}O_{2.95}$ and replace Zr^{4+}, since their ionic radius is close to each other. The defect chemical reaction [30] can be written by Kroege–Vink notations as:

$$ZnO \xrightarrow{BaZrO_3} Zn''_{Zr} + V_O^{\bullet\bullet} + O_O$$

Rietveld refinement of the XRD data showed the BZCY3–Z2 material existed as cubic in the space group Pm3m. The lattice parameters and cell volumes were given in Table 2.

3.4. Electrical conductivity of BZCY3–Z series electrolyte materials

Fig. 6 shows the electrical conductivity measured in humidified hydrogen for BZCY3–Z series electrolyte materials. All the materials exhibit apparent Arrhenius-type temperature dependencies of

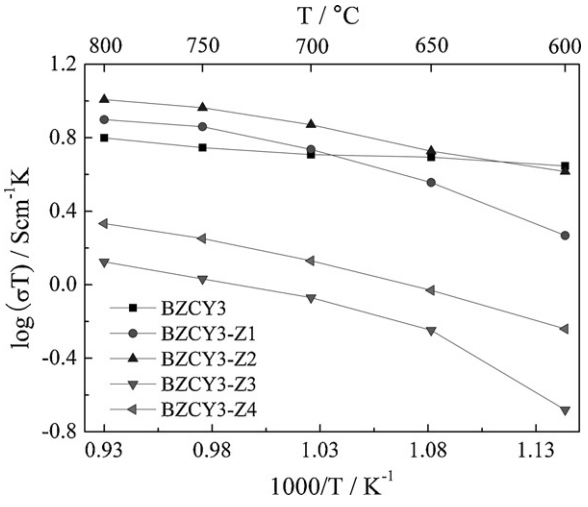

Fig. 6. The influence of ZnO content on the conductivities of BZCY3–Z series composites.

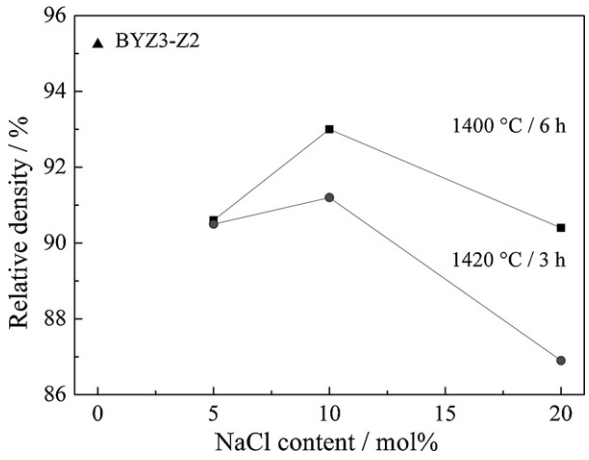

Fig. 7. The relationship between relative densities vs. NaCl content for the BZCY3–Z2–Cl series proton conductors sintered at different conditions.

the total conductivity. The conductivity of sample with 2 mol% of ZnO is 9.27×10^{-3} S/cm at 800 °C, which is higher than that of others. When ZnO content is more than 2 mol%, the total conductivity decreases fast, even lower than that of BZCY. The decrease in conductivity at elevated ZnO content was already observed previously [20,24,30]. Actually, the effects of ZnO as a sintering aid on proton conduction of zirconates and cerates are not very clear [4,20,24,30]. According to Babilo [4], the ionic radius of Zn^{2+} (R^{IV} = 0.074 nm) is close to that of Zr^{4+} (R^{IV} = 0.079 nm). Zn^{2+} can replace Zr^{4+}, causing two negative charges. The negative charges could combine with H^+. As a result, the proton concentration dropped. Meanwhile, the migration of proton might slow down due to this negative charge effect which could also result in low conductivity. Peng et al. [30] believed that the replacement of Zr^{4+} with Zn^{2+} was beneficial for increasing the oxygen vacancy and improving the migration rate of proton. Thus the electrical conductivity increased. Wang et al. [24] attributed a decreased conductivity to Ba loss as x or y raised for $BaCe_{0.5}Zr_{0.3}Y_{0.2-x}Zn_xO_{2.9-0.5x}$ and $BaCe_{0.5}Zr_{0.3}Y_{0.2}O_{2.9} + yZnO$ samples. Zhang et al. [20] believed that part of ZnO existed at the grain boundary and a small part of ZnO dissolved into the lattice of $Ba_{1.03}Ce_{0.5}Zr_{0.4}Y_{0.1}O_{3-\delta}$, which should be responsible for the increase in bulk conductivity. Besides, ZnO existed at the grain boundary could enhance the grain boundary conductivity.

The results shown in Fig. 6 are very close to those reported by Lv et al. [31]. They prepared $BaCe_{0.45}Zr_{0.45}M_{0.1}O_{3-\delta}$ (M = In, Y, Gd, Sm) by conventional sintering at 1600 °C. The sample doped with Y exhibited the highest proton conductivity of 1.06×10^{-2} S/cm at 800 °C. In the present work, 2 mol% of ZnO was used as the sintering aid and to lower the sintering temperature to 1450 °C. However, the conductivities obtained from the two cases were almost in the same level.

As shown in Fig. 6, the samples with low amount of ZnO (1 or 2 mol%) exhibited similar or even a little bit higher conductivity compared with BZCY3, due to the enhancement of densification. It is also observed that the sample with 2 mol% of ZnO had the highest conductivity among all the samples. However, it is clear that excessive ZnO inclusion (≥3 mol%) is harmful to proton conductivity. The reason has been discussed in the previous part of this section.

3.5. Densification and microstructure of BZCY3–Z2–Cl series electrolyte materials

Fig. 7 presents the relationship between relative densities and NaCl content. Obviously, the density of the composite electrolyte materials is lower than that of BZCY3–Z2. Weight loss for BZCY3–Z2–Cl series samples after sintering was observed. In addi-

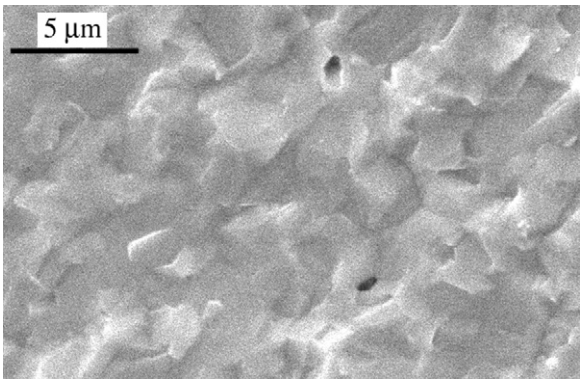

Fig. 8. Fracture surface of sample BZCY3–Z2–Cl10 sintered at 1400 °C for 6 h.

tion, the density of NaCl is lower than that of the composite. All of these resulted in the decrease of the density of final composite electrolyte materials. As shown in Fig. 7, the addition of 10 mol% of NaCl helps to obtain the highest density. Excessive amount of NaCl caused a sharp decrease in density. It can also be seen that the sintering condition of 1400 °C/6 h is better than 1420 °C/3 h. This means that low sintering temperature can avoid the evaporation of NaCl.

The fracture surface of BZCY3–Z2–Cl10 sintered at 1400 °C for 6 h is shown in Fig. 8. Some big pores exist in the BZCY3–Z2–Cl10 sample primarily due to the unavoidable vaporization of NaCl during sintering. The grain boundary is obscure because the grains are surrounded by the molten NaCl. EDS analysis demonstrated that Na was not detected inside the grains but around the grains. It means NaCl mostly distributed along the grain boundary. Compared with other series, it is clear that BZCY3 sample has the smallest grain size and largest amount of grain boundary.

3.6. Influence of NaCl addition on electrical conductivity of composite electrolyte materials

Fig. 9 shows the Arrhenius plots of the total conductivity for the BZCY3–Z2–Cl series electrolyte materials tested in wet H_2 atmosphere. The conductivity increased with increasing temperature, revealing the typical features of ionic conductivity. BZCY3–Z2–Cl10 composite with 10 mol% of NaCl exhibited a conductivity of 1.26×10^{-2} S/cm at 800 °C, much higher than others. That means this material is quite promising for practical applications. However,

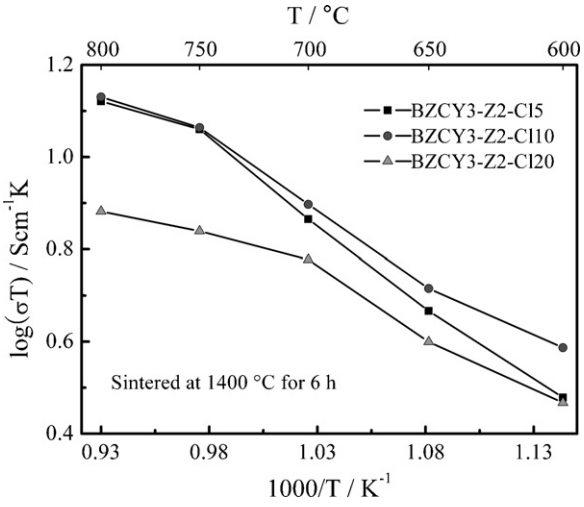

Fig. 9. The influence of NaCl content on the conductivities of samples.

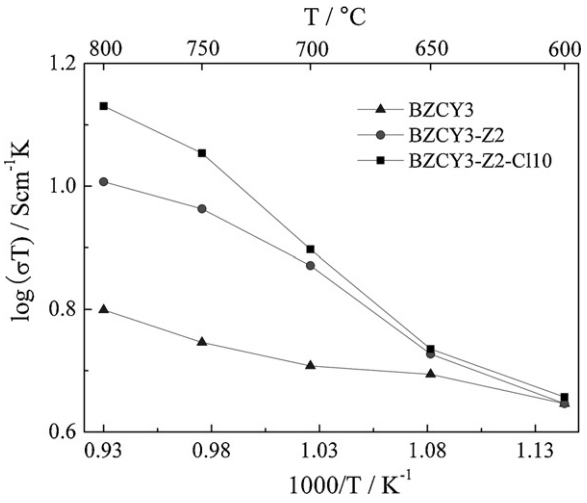

Fig. 10. Conductivity of BZCY3, BZCY3–Z2 and BZCY3–Z2–Cl10 in wet hydrogen.

electrical conductivity decreased dramatically with increasing the content of NaCl.

Fig. 10 shows the conductivity curves of BZCY3, BZCY3–Z2 and BZCY3–Z2–Cl10. Their conductivities are close to each other at 600 °C and increase with increasing temperature. The differences of the conductivity among the three samples become more significant at higher temperature. The conductivity of BZCY3–Z2–Cl10 is 1.26×10^{-2} S/cm, which is much higher than that of others. For example, it is 0.6 orders of magnitude higher than that of BZCY3 (5.87×10^{-3} S/cm) at 800 °C. It is evident that the conductivity of the sample doped with 10 mol% NaCl is good enough for practical applications.

Zhu et al. [32–34] reported a lot of research work on proton conductors doped with inorganic salts, mainly focusing on ceria and cerates. Y doped barium cerate or Ga doped ceria heterogeneous composites were prepared and a high proton conductivity was achieved. The conductivities of 0.01–1 S/cm were obtained at 400–700 °C. Peng et al. [12] reported $BaZrO_3$/NaOH composite proton conductor by conventional sintering. A small amount of ZnO was employed as sintering aid. The total conductivity increased almost by 0.5 orders of magnitude when 40 mol% of NaOH was added in the testing temperature range from 600 °C to 800 °C. At 800 °C, a conductivity of 2.8×10^{-3} S/cm was obtained. It is commonly recognized that NaOH distributed along the grain boundary and helped proton transfer along the grain boundary. In this work, NaCl with proton conduction was utilized to enhance conductivity of barium zirconate by the same mechanism. It can be seen from Fig. 9 that addition of only 10 mol% of NaCl resulted in a conductivity of 1.26×10^{-2} S/cm.

The activation energy and pre-exponential factor listed in Table 3 were obtained from the Arrhenius plots of total conductivities for the composite proton conductors. The activation energy decreases from 0.27 eV for the BZCY3–Z2–Cl5 to 0.17 eV for the BZCY3–Z2–Cl20. The activation energy data demonstrates that the salt could reduce the grain boundary barrier and promote the proton migration. Tao and Meng [27] reported that the defects in pure NaCl are in the form of Schottky pairs, i.e., Na^+ and Cl^- vacancies [35],

$$\text{null} \Leftrightarrow V'_{Na} + V^{\bullet}_{Cl}$$

Therefore, it is expected that the addition of NaCl increases the vacancies and improves the migration of H^+. It is reported that NaCl itself is a very good proton conductor [27]. The NaCl sample sintered at 850 °C for 2 h was coated with Pt paste as the electrode. It was assembled into a fuel cell as electrolyte and the current

Table 3
Activation energy and pre-exponential factor of BZCY3–Z2–Cl as a function of NaCl content.

Sample	BZCY3–Z2	BZCY3–Z2–Cl5	BZCY3–Z2–Cl10	BZCY3–Z2–Cl20
log A (K S/cm)	6.49	4.07	3.61	2.78
E_a (Ev)	0.38	0.27	0.23	0.17

density of the fuel cell reached 70 mA/cm^2. When NaCl was introduced into the BZCY3–Z2 sample, it reinforced the proton conduction for the BZCY3–Z2 sample. The molten NaCl dispersed along the grain boundary could accelerate the H^+ transferring rate, resulting in the decrease of grain boundary resistance.

The decrease of grain boundary resistance with increasing test temperature could also be proved by AC impedance testing as shown in Fig. 11. Due to the limitation of frequency of the electrochemical workstation, the whole curves cannot be given. According to "brick layer" model [36,37], the first (high frequency) semicircle of the AC impedance spectra corresponds to the bulk response and the second semicircle is attributed to the grain-boundary polarization. The third semicircle is related to the processes occurring at the electrodes. In the testing temperature range the first semicircle cannot be resolved because of the frequency limitation of the electrochemical analyzer. However, the bulk resistance can be determined from the high-frequency intercept of the spectrum with the real axis. It can be seen from Fig. 11 that the second arc became more and more apparent and the intercept of the arc with the real axis decreased with increasing temperature. The resistance of grain boundary is about 220 Ω at 400 °C. This implies that NaCl dispersed at the grain boundary enhanced proton migration and decreased grain boundary barrier.

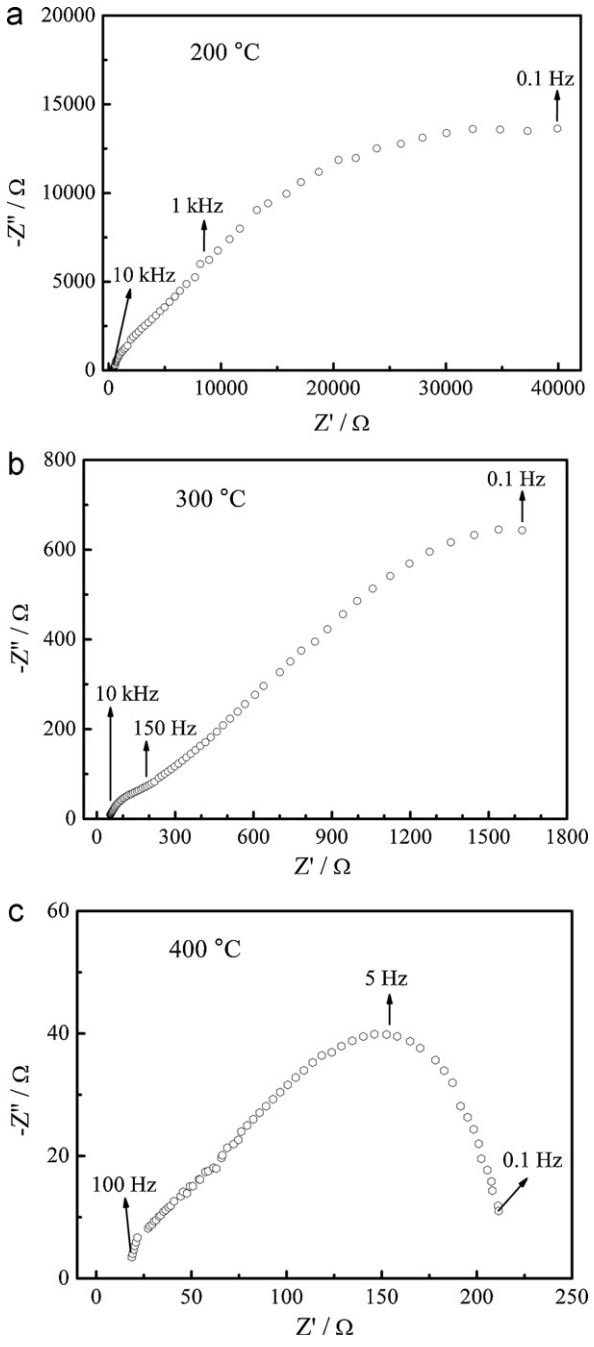

Fig. 11. Impedance spectra of BZCY3–Z2–Cl10 collected at different temperatures.

4. Conclusions

$Ba(Zr_{1-x}Ce_x)_{0.9}Y_{0.1}O_{2.95}$/NaCl ($x$ = 0.1, 0.2 and 0.3) composite electrolyte materials were prepared by solid-state reaction with ZnO as the sintering aid. The sinterability of BZCY series was improved by the addition of ZnO. A small amount of ZnO (1–2 mol%) did not reduce the conductivity of BZCY3–Z. The density of composite proton conductors decreased with the inclusion of NaCl. The electrical conductivity of BZCY3–Z2–Cl10 composite with 10 mol% of NaCl was 1.26×10^{-2} S/cm at 800 °C, which was 0.6 orders of magnitude higher than that of BZCY3. Its activation energy was 0.23 eV, lower than 0.38 eV for the sample BZCY3–Z2. The results indicate that the salt could lower the grain boundary barrier and promote the proton migration.

Acknowledgements

This work was supported by the National Natural Science Foundation of China under grant no. 50872090, no. 51175726 and no. 51072130 and Guizhou province-university scientific and technological cooperation program no. [2011] 7002.

References

[1] F. Iguchi, T.Y. amada, N. Sata, T. Tsurui, H. Yugami, Solid State Ionics 177 (2006) 2381–2384.
[2] R.B. Cervera, Y. Oyama, S. Miyoshi, K. Kobayashi, T. Yagi, S. Yamaguchi, Solid State Ionics 179 (2008) 236–242.
[3] S.B.C. Duval, P. Holtappels, U.F. Vogt, E. Pomjakushina, K. Conder, U. Stimming, T. Graule, Solid State Ionics 178 (2007) 1437–1441.
[4] P. Babilo, S.M. Haile, J. Am. Ceram. Soc. 88 (2005) 2362–2368.
[5] K. Asano, Y. Tominaga, Y. Mugikura, T. Watanabe, Solid State Ionics 181 (2010) 236–239.
[6] C. Vaquero-Aguilar, M.J. López-Robledo, J. Martínez-Fernández, C. Real, M. Jiménez-Melendo, J. Eur. Ceram. Soc. 31 (2011) 1333–1338.
[7] Z.T. Tao, Z.W. Zhu, H.Q. Wang, W. Liu, J. Power Sources 195 (2010) 3481–3484.
[8] F. Iguchi, Y. Nagaoa, N. Sata, H. Yugamia, Solid State Ionics, doi:10.1016/j.ssi.2010.05.046.
[9] Y.B. Kim, T.M. Gür, S. Kang, H.J. Jung, R. Sinclair, F.B. Prinz, Electrochem. Commun. 13 (2011) 403–406.
[10] A. Sin, B.E. Montaser, P. Odier, F. Weiss, J. Am. Ceram. Soc. 85 (2002) 1928–1932.
[11] T. Schober, H.G. Bohn, Solid State Ionics 127 (2000) 351–360.
[12] Z.Z. Peng, R.S. Guo, Z.G. Yin, J. Li, S. Cai, Rare Met. Mater. Eng. 36 (S2) (2007) 596–598.
[13] X.X. Xu, S.W. Tao, J.T.S. Irvine, J. Solid State Chem. 183 (2010) 93–98.
[14] W.P. Sun, L.T. Yan, Z. Shi, Z.W. Zhu, W. Liu, J. Power Sources 195 (2010) 4727–4730.
[15] J.S. Park, J.H. Lee, H.W. Lee, B.K. Kim, Solid State Ionics 181 (2010) 163–167.

[16] Z.W. Zhu, W.P. Sun, L.T. Yan, W.F. Liu, W. Liu, Int. J. Hydrogen Energy 36 (2011) 6337–6342.
[17] D.K. Lim, C.J. Park, M.B. Choi, C.N. Park, S.J. Song, Int. J. Hydrogen Energy 35 (2010) 10624–10629.
[18] J.L. Yin, X.W. Wang, J.H. Xu, H.T. Wang, F. Zhang, G.L. Ma, Solid State Ionics 185 (2011) 6–10.
[19] S.Q. Zhang, L. Bi, L. Zhang, Z.T. Tao, W.P. Sun, H.Q. Wang, W. Liu, J. Power Sources 188 (2009) 343–346.
[20] C.J. Zhang, H.L. Zhao, N.S. Xu, X. Li, N. Chen, Int. J. Hydrogen Energy 34 (2009) 2739–2746.
[21] D.Y. Gao, R.S. Guo, Mater. Lett. 64 (2010) 573–575.
[22] D.Y. Gao, R.S. Guo, J. Alloys Compd. 493 (2010) 288–293.
[23] Y.M. Guo, R. Ran, Z.P. Shao, Int. J. Hydrogen Energy 35 (2010) 5611–5620.
[24] H. Wang, R.R. Peng, X.F. Wu, J.L. Hu, C.R. Xia, J. Am. Ceram. Soc. 92 (2009) 2623–2629.
[25] H.G. Bohn, T. Schober, J. Am. Ceram. Soc. 83 (2000) 768–772.
[26] W. Suksamai, I.S. Metcalfe, Solid State Ionics 178 (2007) 627–634.
[27] S.W. Tao, G.Y. Meng, J. Mater. Sci. Lett. 18 (1999) 81–84.
[28] B. Zhu, Solid State Ionics 125 (1999) 397–405.
[29] M. Oishi, S. Akoshima, K. Yashiro, K. Sato, J. Mizusaki, T. Kawada, Solid State Ionics 179 (2008) 2240–2247.
[30] Z.Z. Peng, R.S. Guo, Z.G. Yin, J. Li, J. Am. Ceram. Soc. 91 (2008) 1534–1538.
[31] J.D. Lv, L. Wang, D. Lei, H.X. Guo, R.V. Kumar, J. Alloys Compd. 467 (2009) 376–382.
[32] B. Zhu, B.E. Mellander, J. Power Sources 52 (1994) 289–293.
[33] B. Zhu, B.E. Mellander, Solid State Ionics 77 (1995) 244–249.
[34] B. Zhu, J. Power Sources 114 (2003) 1–9.
[35] R.W. Dreyfus, A.S. Nowick, J. Appl. Phys. 33 (1962) 473–477.
[36] T. van Dijk, A.J. Burggraaf, Phys. Status Solidi A 63 (1981) 229–240.
[37] M.J. Verkerk, B.J. Middelhuis, A.J. Burggraaf, Solid State Ionics 6 (1982) 159–170.